Secondary structure in solution of two anti-HIV-1 hammerhead ribozymes as investigated by two-dimensional ^{1}H 500 MHz NMR spectroscopy in water

Ramswamy H. Sarma[a,*], Mukti H. Sarma[a], Robert Rein[b], Masayuki Shibata[b], Robert S. Setlik[b], Rick L. Ornstein[b,**], A. Latif Kazim[b], Alfred Cairo[b], Thomas B. Tomasi[b]

[a]*Institute of Biomolecular Stereodynamics, Chemistry Building, State University of New York at Albany, Albany, NY 12222, USA*
[b]*Roswell Park Cancer Institute, Buffalo, NY 14263, USA*

Received 16 November 1994; revised version received 1 December 1994

Abstract Two hammerhead chimeric RNA/DNA ribozymes (HRz) were synthesized in pure form. Both were 30 nucleotides long, and the sequences were such that they could be targeted to cleave the HIV-1 *gag* RNA. Named HRz-W and HRz-M, the former had its invariable core region conserved, the latter had a uridine in the invariable region replaced by a guanine. Their secodary structures were determined by 2D NOESY ^{1}H 500 MHz NMR spectroscopy in 90% water and 10% D_20, following the imino protons. The data show that both HRz-M and HRz-W form identical secondary structures with stem regions consisting of continuous stacks of AT and GT pairs. An energy mimimized computer model of this stem region is provided. The results suggest that the loss of catalytic activity that is known to result when an invariant core residue is replaced is not related to the secondary structure of the ribozymes in the absence of substrate.

Key words: HIV-1 hammerhead ribozyme; HIV-1 gag RNA; 2D NMR; DNA/RNA chimeric ribozyme; GT pair; Imino excited 2D NOESY in water

1. Introduction

In recent years the study of hammerhead ribozymes (HRz) has reached a point where it is possible to design and construct synthetic oligonucleotides which display endonuclease activity against specific nucleic acid targets. Various HRz's were designed to inhibit the expression of HIV-1 RNAs aimed at several different targets, such as a long terminal repeat RNA [1], a 5′ leader/*gag* region [2], and the R region [3]. These efforts are a direct consequence of the pioneering work of Sarver et al. [4] who demonstrated that the HRz's directed against HIV-1 *gag* RNA showed precise cleavage; human cells can stably express the designated HRz, resulting in a substantial reduction in the level of HIV-1 *gag* RNA. It is now well established that the HRz is a potentially valuable therapeutic agent against AIDS, and Sarver, Rossi and their co-workers have presented various specific aspects in recent articles [5,6].

In order to develop a rational modus operandi to combat AIDS pathogenesis through intelligent ribozyme engineering, one must know the 3D structure of anti-HIV-1 HRz's and their substrate complexes. We have selected a chimeric RNA/DNA HRz motif of 30 nucleotides long, as described by McCall et al. [7]. The sequence of this HRz was modified to be complementary to the target region of the HIV-1 *gag* RNA. The HRz will accommodate a 17-mer sequence corresponding to a portion of *gag* HIV-1 RNA. As a first step toward achieving our goal we have determined the secondary structure of two HRz's (HRz-W and HRz-M), the sequences of which are shown in Fig. 1. HRz-W has all the invariant core residues intact. In HRz-M, a uridine in the invariant region of HRz-W was replaced by a guanine nucleotide.

2. Materials and methods

2.1. Synthesis of the 30-mer HRz-M, HRz-W and the 17-mer DNA substrate

The oligonucleotides shown in Fig. 1 were synthesized in the Biopolymer Facility at RPCI on controlled pore glass supports using an Applied Biosystems Inc. model 394 four column DNA/RNA synthesizer and phosphoramdite monomers protected at the 5′ end with the dimethoxytrityl (DMT) group. RNA monomers were additionally protected at the 2′-OH with the *t*-butyl dimethyl silyl group. The synthesis of chimeric DNA/RNA oligonucleotides was accomplished in a stepwise fashion. First, the synthesis of the 3′ end flanking DNA was performed, leaving the product uncleaved from the solid support and with its 5′ end protected with DMT (trityl-on synthesis). Trityl-off RNA synthesis was then performed, creating a chimeric DNA/RNA. Following synthesis, the chimeric DNA/RNA was cleaved from the support and deprotected using ammonia/ethanol (3:1) for 12 h at 55°C. The 2′-*t*-butyl dimethyl silyl protecting group was then removed by treatment with 1 M tetrabutyl ammonium fluoride in tetrahydrofuran (10 ml per OD_{260} unit) for 18 h at ambient temperature. The product was dried and then desalted on a Polypak C-18 cartridge to remove tetrabutyl ammonium salts [7]. The desalted products were analyzed by capillary electrophoresis on an Applied Biosystems Inc. model 270-A HT Capillary Electrophoresis System, using MICRO-GEL$_{100}$ gel-filled capillaries at 35°C. The running buffer was Tris-phosphate (75 mM, pH 7.6, containing 10% methanol), and run times were approximately 20 min at −1 KV. The oligonucleotides were further purified by reverse-phase HPLC using a Waters Instruments model 600 HPLC and VYDAC C-18 (25 × 1 cm) column. A linear gradient (0–100% B in 60 min) of triethyl ammonium acetate (100 mM, pH 7.0, buffer A) acetonitrile (50% in water, buffer B) at a flow rate of 2 ml/min was used to effect separation. The column effluent was monitored at 260 nm using a Waters model 486 variable wavelength detector, and the major fractions were collected, pooled and dried. Sample purity was then again checked by capillary electrophoresis. The synthesis yielded 4.8 mg of Hrz-W and 10.1 mg of HRz-M in pure form.

2.2. NMR spectroscopy

NMR spectroscopy measurements were carried out at 500 MHz at the high field NMR facility for Biomolecular Research, F. Bitter National Magnet Laboratory, MIT. Each of the HRz's was dissolved in 540 ml of H_2O + 60 ml of D_2O, 100 mM in NaCl, 10 mM phosphate

*Corresponding author. Fax: (1) (518) 452-4955.
E-mail: RHS07@CNSVAX.ALBANY.EDU

**Present address:* Molecular Science Research Center, Pacific Northwest Laboratory, Richland, WA 99352, USA.

SSDI 0014-5793(94)01388-8

buffer, pH 7.2. Meausrements were also conducted at a pH of 5.85. The HRz solutions were heated to 80°C and then allowed to cool to 5°C over a period of 4 h. In addition, in the NMR spectrometer, the spectra were taken at 5°C, then the samples were heated to 40°C, and allowed to cool to 5°C over a period of 2 h to record the spectra again. The spectra recorded at 5°C under the above two conditions were identical. Proton NMR spectra in 90% water and 10% D_2O were recorded in the jump-return mode with imino region excitation. The 2D NOESY under the above conditions were recorded using a mixing time of 150 ms in the pure absoption mode [8] with RD of 2 s. The data matrix (2048 × 256) for 128 scans was processed to a size of 2 K × 2 K and analysed using the RNMR program of F. Bitter National Magnet Lab, MIT, developed by David Ruben.

3. Results and discussion

3.1. Presence of multiple species and conformations: identification of the imino resonaces from the dominant conformation.

When a 30 nucleotide long chimeric DNA/RNA HRz (Fig. 1) is suspended in solution one expects the chain to engage in several inter- and intramolecular interactions. In fact, Heus et al. [9] have already demonstrated that ribozymes form several alternate structures, particularly involving GC pairs. In Fig. 2 is shown the imino region of the 500 MHz spectra of HRz-M in the temperature range of 5–30°. In the imino region NMR spectra, in general, the hydrogen bonded iminos of AT and AU pairs appear approximately between 15 and 13 ppm; hydrogen bonded iminos of GC pairs approximately between 13 and 12 ppm; approximately in between 11 and 9.5 ppm appear hydrogen bonded iminos of GT pairs and the non-hydrogen bonded iminos of hairpin regions. However, there are no clear demarcations because the boundaries of the various regions can overlap and it is imprudent to assign the iminos based upon chemical shifts alone. There are clear signatures for various types of base pairing, and, as it will become clear later, we have employed these signatures to assign the signals to different base pairs. In the following, 'AT' and 'GT' terms are used to designate base pairs during general discussion. However, during the discussion of specific pairs in the chimeric DNA/RNA ribozyme, the DNA residues are noted in uppercase and the RNA residues in lowercase.

The spectra shown in Fig. 2 were recorded at a pH of 5.85. When the spectra were recorded at pH 7.2, the resonances in the region of 13.5–15 ppm and those in the 11.5–10 ppm were very broad due to fast exchange at the higher pH. Lower pH was employed to slow down the rate of exchange of the iminos from these regions, and the sharp resonances in the entire imino region at pH 5.85 clearly indicate that the system is amenable to study by NMR spectroscopy.

The extensive number of resonances observed at 5°C, pH 5.85, clearly shows that this cannot be explained on the basis of a single secondary structure for the employed sequence (Fig. 1) and there must be mutiple species. For example, in the AT base pair region (15–13 ppm), at 5°C there are 5 resonances with unequal areas; there are minor resonances in this region, in addition to broad ones. As the temperature is raised from 5 to 10 and then to 15°C, new minor resonances emerge in the AT region, and the broad resonance becomes sharper. At 15°C, there is a total of six resonances suggesting six AT/AU pairs. In the GC base pair region (13–12 ppm), there are minor and major resonances, and area wise, compared to the AT region, the GC region corresponds to about seven base pairs. The

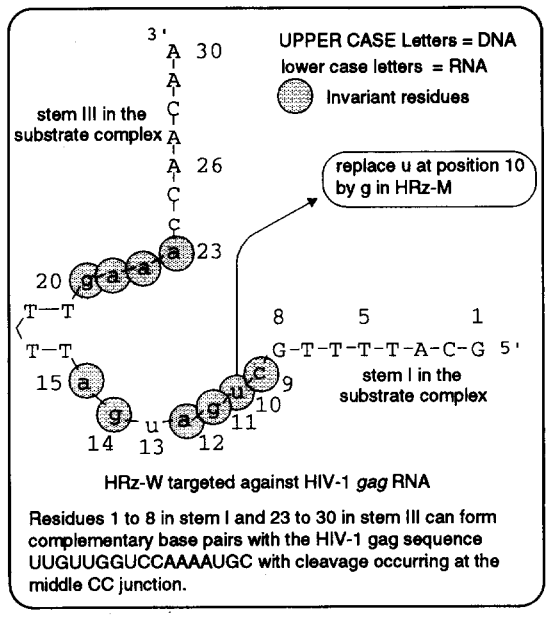

Fig. 1. Sequence of the two hammerhead chimeric DNA/RNA ribozymes HRz-W and HRz-M which can be targeted against the *gag* region of HIV-1.

sequence shown in Fig. 1, under no circumstances, can support a single secondary structure with six AT/AU and seven GC pairs. Obviously these signals arise from the presence of aggregation and multiple species. Particularly interesting to note is that in the temperature range of 25–30°C, a majority of GC pairs begin to 'melt' (broadening of the signals) while the signals from the AT pairs remain sharp, even though regular GC pairs are expected to be considerably more stable than AT pairs, provided they occur in the same conformation, i.e. what is observed will not be the case if all the observed base pairs originate from the same single molecular conformation. We have attempted to remove the aggregation effect at 5°C by diluting the solution by a factor of two; but this had no dominant effect on the spectra. However, when the HRz-M solution was titrated against the 17-mer DNA substrate (Fig. 1) to form an abortive HRz-M–DNA substrate complex, there was clear indication of the progressive disapperance of the resonances from the aggregations as more and more of the abortive HRz-M–DNA substrate complex was generated by base pair formation in the stem I and III region (data not shown, structure of this ribozyme-abortive DNA substrate complex will be reported at a later date).

We have employed temperature elevation to melt out most of the aggregations and to identify the imino resonances at 5°C that originate only from the stable intramolecular secondary structure. As is illustrated in the temperature profile in Fig. 2, elevation of temperature had a pronounced effect on the spectra, particularly at temperatures beyond 15°C. One clearly sees disappearance of several resonances and final emergence of sharp peaks. The iminos that belong to the stable intramolecular secondary structure are marked by residue numbers (later we discuss the assignment of resonances to specific residues) and those belonging to aggregations and minor species are marked by asterisks. Note that the dominant aggregation involves the formation of GC pairs. This aggregation of

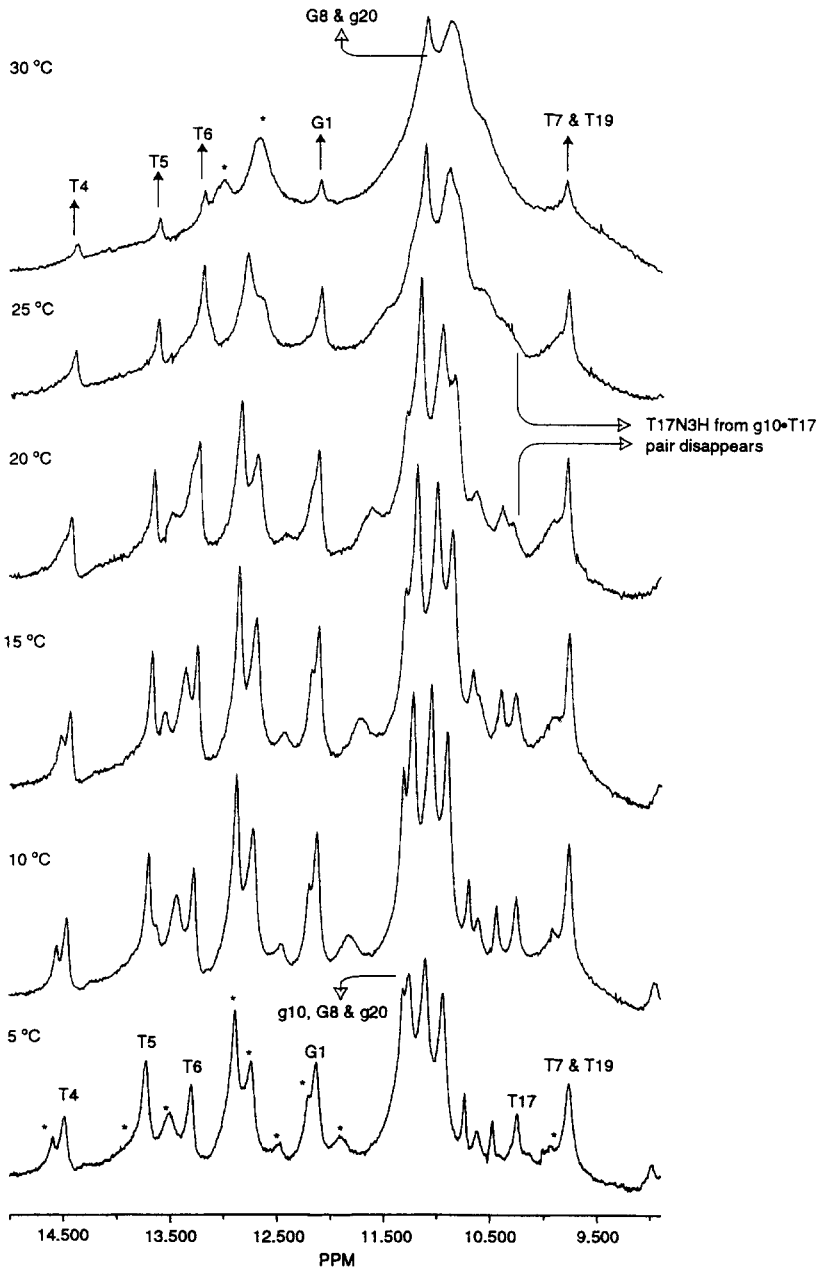

Fig. 2. Temperature profiles of the imino region of the 500 MHz proton spectra of HRz-M, 5°C, pH 5.85. This and the remaing spectra chemical shifts are reported with respect to TSP as an internal standard; uppercase = DNA residues; lowercase = RNA residues. When a resonance is marked T, G or g, it means that the imino signal originates from TN3H, GN1H and gN1H, respectively.

ribozymes by GC pair formation has also been observed by Heus et al. [9].

3.2. *Presence of a track of three AT pairs as a continuous stack in the ribozyme*

The sequence of HRz-M and HRz-W have a track of 4 T's, residues 4, 5, 6 and 7 in Fig. 1, which could form AT pairs with the track of three adenine's at positions 21, 22 and 23. There are two independent lines of evidence which support the formation of a continuous stack of three a·T pairs (lowercase = RNA; uppercase = DNA). (i) In Fig. 3 we show the NOESY cross- peaks between the various imino resonances. Here note the cross-peaks, marked **a** and **b**, between residues T4 and T5 and that between residues T5 and T6. These cross-peaks in the AT region, for the sequence under study, can be explained only on the basis of a continuous stack of three AT pairs with inter base pair magnetization transfer, i.e. magnetization is transferred from the TN3H of T4·a23 pair to the TN3H of T5·a22 from where it is transferred to the TN3H of T6·a21. In an RNA type stack the distance among the adjacent TN3H's is about 3.7–3.8 Å. (ii) In Fig. 4 we show the NOESY plot showing the magnetization transfer from the imino region to the non-excahgeable aromatic region. The region marked **a** in the diagram is a typical signature of a continuous stack of three AT pairs which display both intra base pair and inter base pair magnetization transfer. What happens can be best summarized in the case of

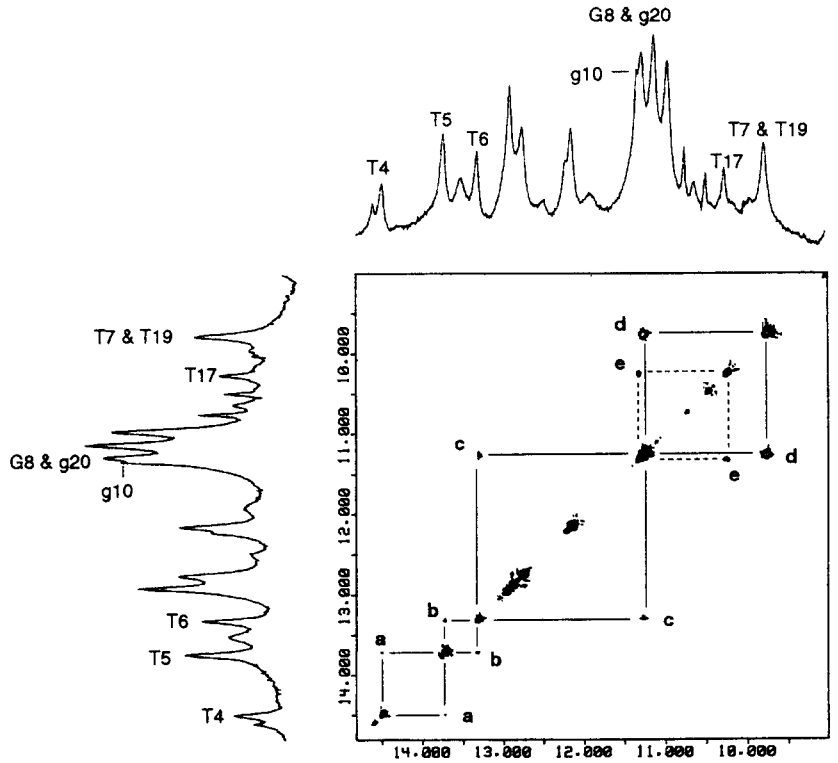

Fig. 3. Contor plot of 2D NOESY 500 MHz spectrum (5°C, pH 5.85) showing the cross-peaks between the imino protons in HRz-M. See text for explanations of cross-peaks marked **a**, **b**, **c**, **d** and **e**.

transfer from T5N3H in the stack: from the TN3H of T5·a22, there is an intra base pair transfer to a22H2 (distance 2.5–2.8 Å, very strong cross-peak, in fact this is an unmistakable signature of an AT pair), there are also two inter base pair transfers, one to a23H2 (distance ~4 Å, medium strong cross-peak) and another to a21H2 (distance ~5.5 Å, weak cross-peak). In the case of T4N3H we see transfer to a23H2 and to a22H2. In this region, T6N3H transfers magnetization to a21H2 and a22H2.

Given the sequence in Fig. 1, the observed cross-peaks (Figs. 3 and 4) associated with the imino resonances in the AT region can be rationalized only on the basis of the above assignments that emerge out of a continuous stack of three AT pairs in the secondary structure.

3.3. *The presence of four GT pairs in the secondary structure of HRz-M*

Once a continuous stack of AT pairs are incorporated into the secondary structure, the remaining elements of the structure automatically falls in place as shown in Scheme 1. This secondary structure contains four GT pairs. GT pairs normally occur in the 11–9.5 ppm region and they have their individual signature in the form of an intra base pair cross-peak between GN1H and TN3H, a distance between them of ~2.5 Å. These are very clearly seen in Fig. 3, in the cross-peaks marked **d** and **e**. Note that cross-peak **d** is very strong, and originates from T7·g20 and T19·G8 pairs. The chemical shifts of TN3H of T7 and T9 and that of GN1H of g20 and G8 overlap. Because of degeneracy in chemical shifts one cannot observe inter base pair NOEs between the two GT pairs. The cross-peak marked **e** has to originate from the T17·g10 base pair. Note that in the proposed secondary structure (Scheme 1) this pair is toward the end of the stem; the T16·g11 pair at the terminus will not normally be observable because of its exchange with the solvent in the loop consisting of residues 12, 13, 14 and 15. One will also expect the TN3H of T17 and G1H of g10 to exchange with the solvent as the temperature is elevated. In fact the temperature profiles in Fig. 2 show that at temperatures beyond 15°C these resonances disappear, as expected.

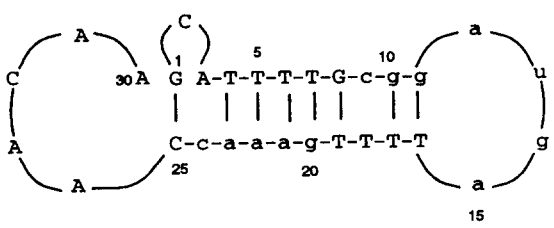

Scheme 1. Secondary structure of HRz-M. Uppercase = DNA residues, lowercase = RNA residues.

3.4. *The continuous stack of three AT pairs is adjacent to the GT stack*

An important feature of the proposed secondary structure is that the GT stack is adjacent to the AT stack; and if this is true one must observe inter base pair NOE transfer between T6·a21 and T7·g20 base pairs. In fact the observation of three cross-peaks (Figs. 3 and 4) associated with this structural feature attests to the correctness of the structure. They are: (i) in Fig. 3, the cross-peak marked **c** which originates from the transfer of NOE between TN3H of T6·a21 base pair to GN1H of T7·g20 base pair (distance ~5 Å); (ii) in Fig. 4, the cross-peak marked **d** which originates from the transfer of NOE between a21H2 and GN1H of g20 (distance ~4.5 Å); (iii) in Fig

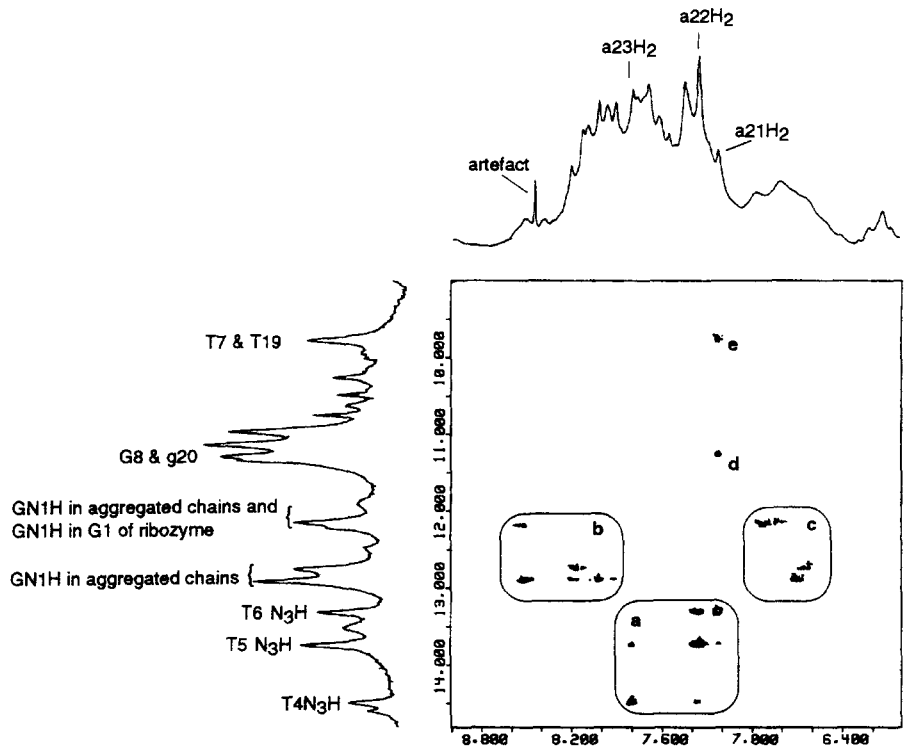

Fig. 4. Contor plot of the 2D NOESY 500 MHz spectrum (5°C, pH 5.85) showing the cross-peaks between imino protons, and non-exchaging and exchanging protons in the 9–6 ppm range. See text for explanations of **a**, **b**, **c**, **d** and **e**.

4, the cross-peak marked **e** which originates from the transfer of NOE between a21H2 and TN3H of T7 (distance ~4.8 Å).

3.5. Presence of a single GC pair in the secondary structure

Examination of the imino region at 30°C indicates the presence of a sharp imino resonance, corresponding to a single proton, in the region where one expects iminos from GC pairs. At 5°C this resonance is buried inside the GC iminos from the aggregations. The resonances can be assigned to GC iminos from GC pairs by examining the transfer of magnetization. In a GC pair, one expects intra base pair transfer of NOE from G1NH to the hydrogen bonded aminos (between 8 and 9 ppm) and to the non-hydrogen bonded aminos (between 6 and 7 ppm). These transfers are observed and are shown in areas marked **b** and **c** in Fig. 4. In addition we have established the cross-connectivity between the hydrogen bonded aminos and the non-hydrogen bonded aminos by plotting the diagonal in the 9–6 ppm range (not shown).

In the sequence of HRz-M within the boundary condition of accommodating 3 AT pairs, and four GT pairs, the only way to accommodate a GC pair is to invoke a bulge between nucleotides 1 and 3 so that a G1·C25 pair can be formed (see Scheme 1).

At elevated temperatures, the resonance from g10·T17 in HRz-M disappears due to fast exchange, suggesting possible enlargement of the loop shown on the right side at elevated temperatures. However, at 30°C we did observe the G1H of a GC pair as fairly sharp, suggesting that the G1·C25 base pair is protected from solvent accessibility, despite the fact that it is located at the end of the helix. This observation suggests that the sequence in the region 26–30 is not a random structure, but folds and stacks against the helix, preventing accessibility of water molecules to the stem terminus.

3.6. Computer modeling of the stem region in the secondary structure of HRz-M

The helical stem was molecular modeled (Fig. 5) according to the NMR secondary structure with the nucleotides assumed to have an A conformation, in accord with the fiber diffraction data of DNA/RNA hybrid duplexes [10,11]. From the results discussed above, the stem region contains two G·T mispairs (g20·T7; G8·T19) and, as described below, the presence of a A3–c24 mispair in the stem is possible, but not confirmed. The G·T mispairs were modeled using the conformation of the G4–U69 pair of $tRNA^{phe}$ as a template [12] while the A3–c24 mispair was modeled according to Sarma et al. [13] in which a single hydrogen bond exists between N1 and N4 of the A and C bases, respectively. C2 was modeled in a bulged conformation to accommodate the G1·C25 pair as described in the preceding section. The molecular modeling of the stem region was accomplished using the SYBYL package (version 5.5; Tripos Associates Inc.) installed on a Evans and Sutherland graphics workstation. Energy minimization was performed using the MAXIMIN2 module of SYBYL with Kollman all-atom parameters for 300 steps of steepest descent and 300 steps of conjugate gradient. The observed various inter proton cross-peaks in Figs. 3 and 4 are entirely consistent with the inter proton distances in the model illustrated in Fig. 5.

3.7. Secondary structure of HRz-W

In the case of HRz-W, the 1D spectra of the imino region and the NOESY pattern from the imino region were extremely

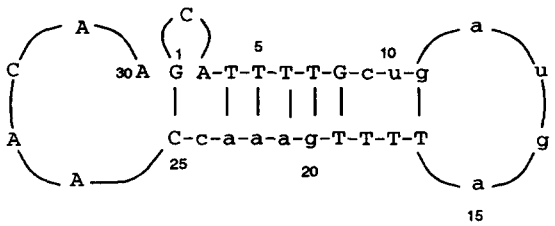

Scheme 2. Secondary structure of HRz-W. Notations, see Scheme 1.

similar to that of HRz-M described above. Analysis of the data in a manner similar to what is described above leads to a secondary structure (Scheme 2) essentially idential to that of HRz-M, the only difference being the absence of a GT pair at the right side of the stem.

In the secondary structure for HRz-M and HRz-W it is possibe to have a single hydrogen bonded A3·c24 pair (under our conditions of pH 5.85, adenine is not protonated). Even though we have detected single hydrogen bonded AC pairs in pure DNA systems [10], we have no evidence for the presence of an A·c pair in the current systems.

3.8. Difference between HRz-M and HRz-W

The only difference in the sequence between HRz-W and HRz-M is that, in HRz-W the invariant core residues are preserved, and in HRz-M a uridine in the core region was replaced by a guanine (Fig. 1). It has been demonstrated that replacement of conserved residues at the core results in substantial loss of catalytic activity [15]. The results in this paper indicate that such a replacement in the current systems does not alter the

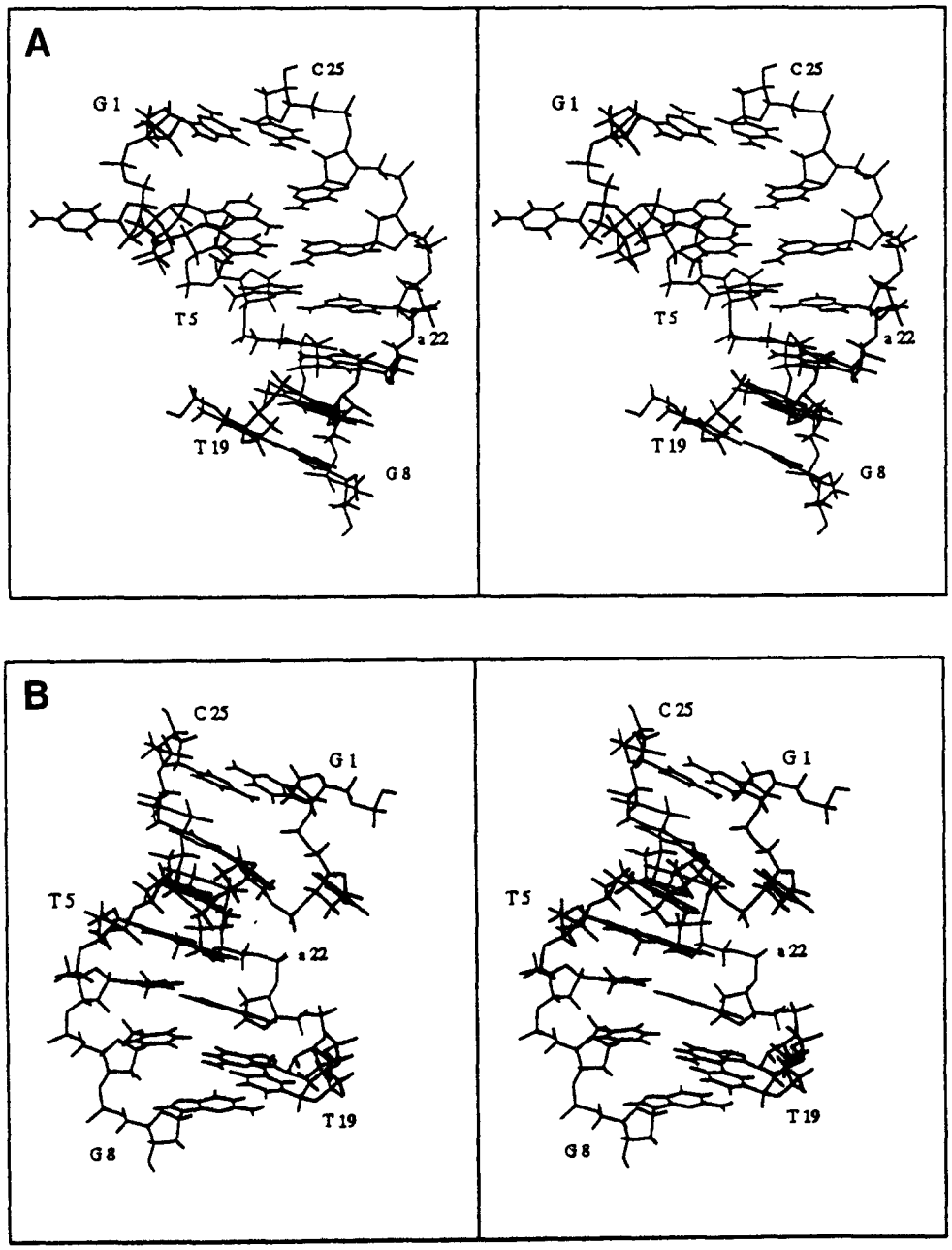

Fig. 5. Stereo view of a molecular model of the stem region of HRz-M. Panel B is a 90° rotation of A. This figure was prepared using the MOLSCRIPT program [14].

secondary structure of the uncomplexed HRz's, and hence it is likely that this differential catalytic activity may be associated with the 3D structure of the HRz's and/or their substrate complexes. Based on fluoresence measurements, the 3D structure of a model hammerhead ribozyme was recently proposed by Tuschl et al. [17], which agreed well with the X-ray structure recently reported by Pley et al. [18]. The X-ray structure suggested an important structural role for the invariant residues in domain 1 (c9, u10, g11, a12 in our system) in forming a sharp turn similar to other loops found in tRNA. In our work, in the absence of substrate, a significant difference on the secondary structure was not observed by the replacement of u10 by g10. From Schemes 1 and 2, it seems clear that the secondary structures observed in our experiments are dominated by the presence of the consecutive AT and GT pairs where the T4–T7 region forms the consecutive base pairs with g20–a23. Since the sequence of the T4–T7 region was chosen to complement the target sequence, it is expected that this region will form standard Watson–Crick pairs with the substrate and not with the ribozyme core region. Thus, in the presence of the substrate, it is anticipated that the formation of stem I will prevent the formation of the consecutive AT and GT pairs observed in our experiment.

However, our secondary structure may raise one interesting question for the design of the pharmaceutical ribozyme, namely the role of ribozyme sequence complementary to the target sequence in the stem I and stem III region. If the ribozyme bases in the stem region interact strongly with the ribozyme core region, it may prevent, or interfere with, the formation of the appropriate secondary and tertiary structure for the ribozyme–substrate complex. Thus, in addition to the question of whether the substrate bases are exposed to form a duplex with ribozyme, the complementarity of the stem region to the ribozyme core structure may have to be taken into account for the optimal design of the therapeutic ribozyme.

Because of extensive overlap of resonances in the D_2O spectrum, and due to the uncertainities involved in the derivation of 3D structures from 2D homonuclear NOESY data [16], efforts are underway in this laboratory to derive the 3D geometry of ribozymes of the anti HIV-1 HRz family and their substrate complexes in solution by employing heteronuclear NMR methods on ^{13}C and ^{15}N enriched samples.

Acknowledgements: This research was supported by National Foundation for Cancer Research, National Institutes of Health (GM 29789), NASA (NAGAW1546) and the Office of Health and Environmental Research of the US Department of Energy (KP0402). The high-field NMR experiments were performed at the NMR Facility for Biomolecular Research located at the F. Bitter National Magnetic Laboratory. The NMR facility is supported by Grant RR00995 from the Division of Research Resources of the NIH and by the National Science Foundation under contract C-67. The technical assistance of Tom Isac, Amy Frechette and Yi Ping Sun in the preparation of the oligonucleotides is gratefully acknowledged.

References

[1] Heidenreich, O. and Eckstein, F. (1992) J. Biol. Chem. 267, 1904–1909.
[2] Homann, M., Tzortzakaki, S., Rittener, K., Sczakiel, G. and Tabler, M. (1993) Nucleic Acids Res. 21, 2809–2814.
[3] Ventura, M., Wang, P., Ragot, T., Perrricaudet, M. and Saragosti, S. (1993) Nucleic Acids Res. 21, 3249–3255.
[4] Sarver, N., Cantin, E.M., Chang, P.S., Zain J.A., Ladne, P.A., Stephens, D.A. and Rossi, J.J. (1990) 1222–1225.
[5] Sarver, N., Black, R.J., Bridges, S. and Chrisey, L. (1992) AIDS Res. Hum. Retroviruses 8, 659–6670.
[6] Sarver, N. and Rossi, J.J. (1993) AIDS Res. Hum. Retroviruses 8, 659–6670.
[7] Vinayak, R. (1993) Chemical synthesis, analysis and purification of oligonucleotides, Methods: A Companion to Methods in Enzymology 5, 8–18.
[8] States, D.J., Haberkorn, R.H. and Ruben, D.J. (1982) J. Magn. Reson. 48, 286–292.
[9] Heus H.A., Uhlenbeck, O.C., and Pardi, A. (1990) Nucleic Acids Res. 18, 1103–1108.
[10] Milman, G., Langridge, R., Chamberlain, M.J. (1996) Proc. Natl. Acad. Sci. USA 57, 1804–1810.
[11] Saenger, W. (1984) Principles of Nucleic Acid Structure, Springer-Verlag, New York.
[12] Hingerty, B.E., Brown, R.S. and Jack, A. (1978) J. Mol. Biol. 124, 523–534
[13] Sarma, M.H., Gupta, G. and Sarma, R.H. (1987) Biochemistry 26, 7707–7715.
[14] Kraulis, P.J. (1991) J. Appl. Cryst. 24, 946–950.
[15] Ruffner D.E., Stormo, G.D. and Uhlenbeck, O.C. (1990) Biochemistry 29, 10695–10702.
[16] Ulyanov, N.B., Gorin, A.A., Zhurkin, V.B., Chen, B.C., Sarma, M.H. and Sarma, R.H. (1992) Biochemistry 31, 3918–3930.
[17] Tuschl, T., Gohlke, C., Jovin, T.M., Westhof, E. and Eckstein, F. (1994) Science 266, 785–789.
[18] Pley, H.W., Flaherty, K.M. and McKay, D.B. (1994) Nature 372, 68–74.